Power dissipation in a capacitive coupled 450 khz discharge set up for a CO_2 laser

J. de la Rosa, J. Corredor, J. Yaljá, F. Gallegos, and P.A. Calva
ESIME-IPN,
07738 México, D.F.,
e-mail: jos_delarosa@yahoo.com.mx

Recibido el 30 de enero de 2007; aceptado el 27 de abril de 2007

In order to find the power dissipation in a 450 kHz capacitive coupled CO_2 laser system using a 50 Ω π matching network, we investigate its electrical behavior. Current and voltage evolution and the phase delay in all the circuit elements were measured with calibrated Rogowski coils and high voltage probes. The signals were registered using a digital oscilloscope interfaced to a PC. When the supplied power lay between 0.5 and 1 kW, the signals had a non-distorted sinusoidal form. This allowed to make the power dissipation estimation in the circuit elements using their current and voltage peak values, and their phase delay. Phase measurements were made with $\pm$ 0.3° accuracy, which gives an accuracy of $\pm$ 1.5% in the laser chamber power dissipation estimation. The laser chamber power dissipation is estimated at between 30 and 50% of the supplied power, and the rest is consumed in the matching circuit. The power losses in the matching circuit greatly contribute to the poor total system efficiency ($\approx$ 0.8%). The estimated resistance and capacitance values of the laser chamber are also presented.

Keywords: Laser; discharge; r.f.

Se investiga el comportamiento eléctrico de un láser de CO_2 excitado a través de una descarga capacitiva de 450 kHz con el fin de determinar la potencia disipada en la cámara de descarga y en la red de acoplamiento entre la fuente de radio frecuencia y la cámara de descarga. Para medir la evolución temporal de la corriente y voltaje, así como el corrimiento de fase entre ambas, en cada elemento del circuito, se usaron bobinas de Rogowski y puntas de alto voltaje calibradas. Las señales fueron registradas en un osciloscopio digital y almacenadas en una PC. Cuando al sistema se suministra potencia entre 0.5 y 1 kW, las corrientes y voltajes en el circuito muestran una evolución sinusoidal no distorsionada, lo que permite una estimación de la potencia disipada en cada elemento usando los valores pico de su corriente y voltaje, y del corrimiento de fase entre ambas. Se realizaron mediciones de fase con una incertidumbre de 0.3°, lo cual genera una incertidumbre de 1.5% en la estimación de la potencia disipada en la cámara de descarga. Se estima que la potencia disipada en la cámara de descarga es del 30 al 50% de la potencia suministrada y el resto se consume en la red de acople, razón por la cual la eficiencia total del láser es muy pobre ($\approx$0.8%). Con las mediciones realizadas se determinó también la resistencia y capacitancia equivalente de la cámara de descarga.

Descriptores: Láser; descargas; r.f.

PACS: 42.60.Lh; 52.80.Pi; 84.37.+q

1. Introduction

Continuous wave (CW) CO_2 lasers can be operated at about 20% efficiencies using direct current (DC) [1,2], radio frequency (RF) [3,4] or microwave (MW) [5] electrical discharges. Because RF or MW discharges do not requiere internal electrodes and do not use ballast resistance, the energy supplied in the discharge volume without arc production (90 W/cm^3 [5,6]) is higher than in DC discharges (10 W/cm^3 [5]), which allows a compact construction of high power CO_2 lasers. While it is possible to obtain a maximum power of 100 W/m with convection cooled DC-CO_2 lasers [2], with diffusion cooled RF or convection cooled MW it is possible to obtain more than 1 kW/m [5-8]. Another reason to promote RF and MW discharges for high power CO_2 lasers is that the lack of internal electrode prevents gas and resonator contamination due to metal sputtering [9]. The disadvantage of the RF (13-200 MHz) and MW (2.45 GHz) technologies, in comparison to DC, is their higher costs. So one option for overcoming this could be the operation of the discharge at lower frequencies. The use of 0.3 to 1 MHz excitation has recently been reported in a low power diffusion cooled CO_2 laser,the so-called slab laser [10]; (using an RF power supply whose impedance is the same as the laser chamber impedance) the authors have obtained an efficiency of about 16% with an electrical input power density of 5 W/cm^3. We investigate here the operation of a convection cooled CO_2 laser excited with a 450 kHz capacitive coupled discharge, using a 50Ω RF power supply.

It is well known [11-13] that a large part of the power delivered by an RF generator in a plasma setup is dissipated in the matching circuit, *i.e.* outside the plasma, and hinders the supply of more energy into the plasma [14]. Power meters are easy to use to characterize the plasma as a function of RF power transmitted to the matching network, but this method may be in serious error due to matcher losses that can account for up to 90% of the measured transmitted power [15]. Calorimetric techniques can be used to calculate the power losses on the matching network and by subtracting this value from the total power, measured with an in-line power meter, the power dissipated by the discharge can be calculated [16-17]. So, the knowledge of the dissipated power in all parts of the setup is useful, not only for finding the efficiency of the system, but for establishing the influence of the components in the behavior of this arrangement. Time-resolved current and voltage measurements on all elements

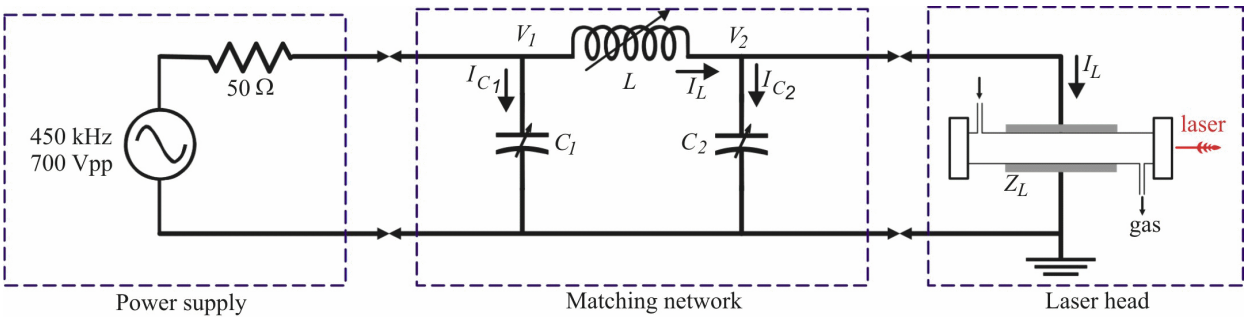

FIGURE 1. Schematic diagram of a 450 kHz capacitive coupled CO_2 laser.

of a set up for plasma excitation are very important on order to find the power consumption of each one. In plasma chambers, where the voltage and current phase is in the order of degrees, these measurements can be taken using oscilloscopes [18] or vector network analyzers [19]. Here we present phase measurements and voltage to current peak value rates in the laser head of a 450 kHz capacitive coupled CO_2-laser using an oscilloscope and a gain and phase detector circuit, measurements which are used to calculate its impedance and its dissipated power.

2. Experimental arrangement

Figure 1 shows a schematic diagram of the RF capacitive coupled CO_2 laser. The laser head consists of a Pyrex tube (280 mm long, 25 mm in external diameter and with a 1.5 mm wall) with external aluminum electrodes (100 mm long and 5 mm wide in the interface electrode-tube) bonded to the tube with Wale bond 15-1483 ceramic paste. Both electrodes are water cooled. The optical resonator, 50 cm in length, is formed with two 2-inch internal mirrors; a 99.9% reflectivity mirror (20 m curvature radius); and a 95% reflectivity plane coupling mirror.

A 35 mbar laser gas mixture CO_2-N_2-He (1:10:11.5) is circulated in the laser chamber at 75 m/s along the optical axis with a Roots pump (Leybold-505). Three heat exchangers in the gas network, cooled by a Caron High Performance Chiller HPC 5.5, are used to keep the gas temperature at 15°C.

The RF generator is a COMDEL CLF 5000/PLL working at a frequency of 450 kHz ± 10 kHz, .05-5 kW_{rms} power, a maximum voltage of 700 V_{pp}, and an output impedance of 50Ω.

The two capacitors, C_1 and C_2, and the coil L of the π impedance matching network can be calculated as follows [20]:

$$C_1 = \frac{\omega^3 \cdot L \cdot C_2^2 + \frac{\omega \cdot L}{Z_L^2} - \omega \cdot C_2}{\omega \cdot \left[(1 - \omega^2 \cdot L \cdot C_2)^2 + \left(\frac{\omega \cdot L}{Z_L} \right)^2 \right]} \qquad (1)$$

$$C_2 = \frac{1}{\omega^2 \cdot L} \left[1 + \sqrt{\frac{R_0}{Z_L}} \cdot \left(1 - \frac{\omega^2 \cdot L^2}{R_0 \cdot Z_L} \right) \right] \qquad (2)$$

and

$$L < \sqrt{\frac{R_0 \cdot Z_L}{\omega^2}}, \qquad (3)$$

where R_0 is the RF generator impedance, Z_L the laser head impedance and ω is the angular frequency, choosing a Z_L of 800 Ω and an L of 15 μH, $C_1 = 39$ nF and $C_2 = 10$ nF. Experimentally, C_1 was adjusted to 79 nF in order to have the minimum back reflection of RF power to the generator.

C_1 was constructed on a copper circuit board with series-parallel (2×34) arrangements of polypropylene Vishay Orange Drop 715P (600 V D-C/ 200 V A-C) 4.7 nF capacitors, whose ESR (Equivalent Series Resistance) is about 1.3 mΩ and their maximum ratings are 200 V_{rms} and 2.62 A_{rms} at 450 kHz [21]. The maximum ratings of the constructed C_1 arrangement were about 400 V_{rms} and 89 A_{rms}.

C_2 was also constructed too on a copper circuit board with series-parallel (14×14) arrangements of polypropylene 10 nF capacitors of the same type, whose ESR is about 0.5 mΩ and their maximal ratings are 100 V_{rms} and 2.83 A_{rms} at 450 kHz [11]. The maximum experimental ratings in our investigation of the constructed C_2- arrangement were 1.4 kV_{rms} and 39.6 A_{rms}, and under laser operation it need to be air cooled.

L is a water cooled spiral coil with equal external diameter and length (135 mm), which gives the minimum resistance effect [22]. It was constructed with 14 turns of commercial copper tube of 4.5 mm external diameter and a 1 mm wall, with a space between adjacent turns about 5.5 mm. The measured resistivity of the tube is of about 3.79×10^{-6}Ωcm (because its surface oxidizes). To avoid the effects of the Lorentz forces, it was mounted on a Plexiglas plate.

The elements of the experimental arrangement were interconnected with 14 AWG copper wire in order to measure the current measurements. Voltage and current were measured in all elements of the circuit using a Tektronix High Voltage Probe P6015A and home made Rogowski coils, whose calibration was done on a pure resistive 50 Ω charge coupled to the RF source. The signals were registered by a 2440 digital Tektronix Oscilloscope. Laser radiation was characterized with a Radiometer Coherent Ultima-10 and a CO_2 Spectrum analyzer from Optical Engineering Inc.

3. Theory

Based on ac circuit theory, the instantaneous power in a circuit element is given by the product of the time dependent current and voltage. The average power over a period T is then given by

$$P = \frac{1}{T}\int_{o}^{T} V(t)\, I(t)\, dt. \tag{4}$$

For a sinusoidal current and voltage, Eq. (4) can be written as

$$P = \frac{V_p I_p}{2}\cos\phi \tag{5}$$

where V_p and I_p are the peak voltage and current in the circuit element and ϕ is the relative phase between then. Because the resistor and the coil in Fig. 1 are not ideal, both could be represented by series LR arrangements, and in this case the phase shift in Eq. (5) can be written as

$$\phi = tg^{-1}\left(\frac{\omega L}{R}\right), \tag{6}$$

where ω is the angular frequency of the ac signal,

$$L = \frac{V_p}{I_p\omega}\left[\left(\frac{1}{tg\phi}\right)^2 + 1\right]^{-1}, \tag{7}$$

and,

$$R = -\frac{\omega L}{tg\phi}. \tag{8}$$

Similarly the capacitors in the setup could be represented by series CR arrangements, and the phase shift can be written as

$$\phi = tg^{-1}\left(\frac{1}{\omega CR}\right), \tag{9}$$

where

$$C = \frac{I_p}{V_p\omega}\left[\left(\frac{1}{tg\phi}\right)^2 + 1\right] \tag{10}$$

and

$$R = \frac{1}{\omega C\, tg\phi}. \tag{11}$$

For coils and capacitors typically used in matching circuits, the phase ϕ is such that the current and voltages are close to 90°. In our setup, a 15 μH inductance for L was measured. Its series resistance due to the skin [23] and proximity effects [24,25] was calculated to be 163 mΩ at 450 kHz. Then, from Eq. (6) and 450 kHz, one obtains the value $\phi = 89.78°$. From Eq. (5),

$$P \approx \frac{V_p I_p}{2}\delta, \tag{12}$$

where $\delta = (\pi/2) - \phi = 0.22°$. Following [26], from Eq. (12) the uncertainty in the power measurement due to uncertainties in the relative phase measurement is given by

$$\frac{\Delta P}{P} \approx \frac{\Delta\delta}{\delta}. \tag{13}$$

For $\Delta P/P$=10%, $\Delta\delta$=0.022°. At a frequency of 450 kHz this means a timing accuracy of approximately 136 ps to achieve an accuracy of 10% in the power measurement, which can not be achieved with an oscilloscope. These requirements are more critical for the voltage and current phase measurements in C_1 and C_2, whose ESR's were estimated to be in the order of 1 mΩ (for C_2, ϕ=89.999°).

Also used was a gain and phase detector circuit based on an AD8302 CI from the firma Analog Devices company, which measures a gain over a $\pm$30 dB range scaled to 30 mV/dB, and of phase over a 0-180° range scaled to 10mV/degree [27]. To have a 0.01° resolution, we use a 2 V, $4\frac{1}{2}$digit DC voltmeter. In order to have minimal uncertainty, we attempted to calibrate the phase detector circuit using a RG58/U coaxial cable, but it was only possible to obtain an accuracy of approximately 0.3°, which is not enough to measure the losses in the elements of the matching network.

However, the 2440 oscilloscope and the phase detector circuit were useful in measuring the voltage and current phase in the laser chamber, where it is in the order of tenths of degrees. Because the laser chamber can be represented by an equivalent series RC circuit [10], the laser chamber power dissipation, its resistance and its capacitance can then be calculated using Eqs. (5), (10) and (11).

4. Experimental results

To fire the discharge at 35 mbar gas pressure, supplied powers below 600 W preionization are necessary. This could be achieved using a Tesla coil. Above that power, the discharge fires automatically. If instead of Pyrex a Teflon tube is used, the discharge does not take place, happens in other capacitive arrangements [28]. This means that, besides the volume ionization of the gas [4], the glass surface electron emission must be considered. It is known that field stimulated "exoelectron emission" from a glass surface into a vacuum is possible when a high voltage step is applied [29].

The homogeneity of the discharge in our arrangement depends on the width of the electrode and on the supplied electrical power. For 5 mm wide electrodes, the luminosity of the discharge fills the face-to-face space between them. The use of wider electrodes concentrates the luminosity between their edges, producing a dark hollow around the optical axis. For 5 mm wide electrodes, the luminous homogeneity increases with the supplied power; for low powers, it is higher at the tube wall.

The electrical and laser emission behaviors of the system are shown in Figs. 2 and 3. Figures 2a and 2b show the peak voltages and currents in all the circuit elements as a function of the generator power for a 35 mbar laser gas mixture. Figure 2c shows the voltage and current phase ϕ in the laser chamber. In L, C_1 andC_2, no appreciable $\Delta\delta$ was detected. After Fig. 2c and Eq. (13), where $\delta = (\pi/2) - \phi$ and $\Delta\phi \approx 0.3^0$, the uncertainty in the calculation of the laser power dissipation would be in the range 1.4%$\leq \Delta$P/P$\leq$1.8%.

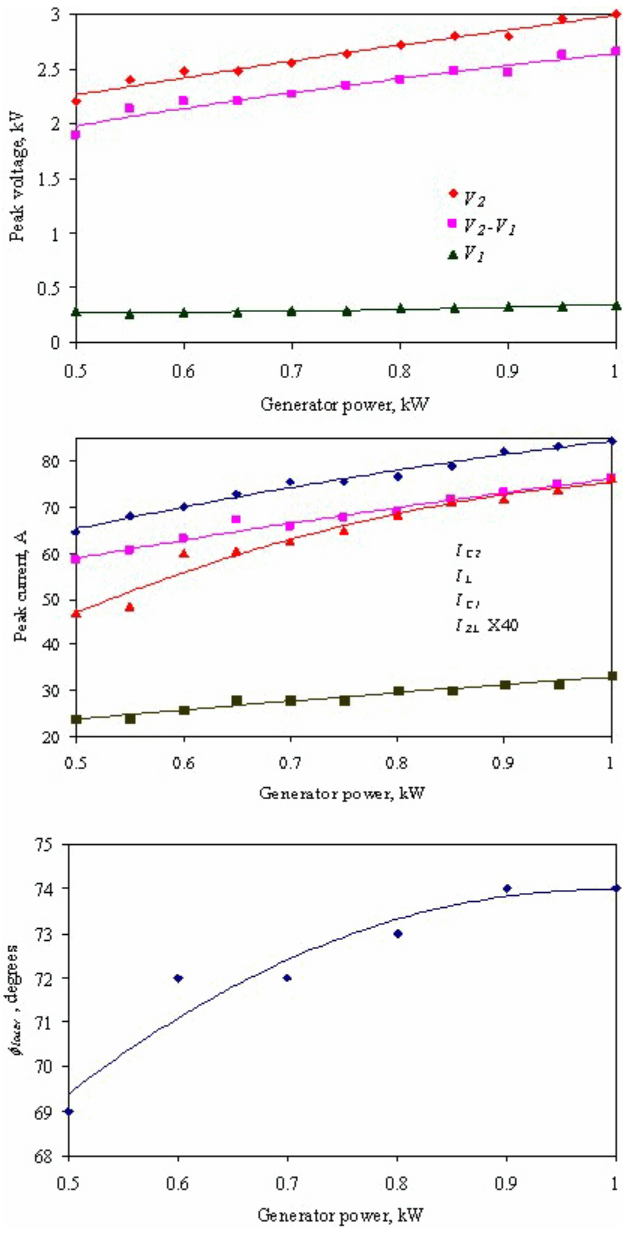

FIGURE 2. Electrical behavior of the CO_2 laser as a function of the supplied power: a) Peak voltages V_1 in C_1, V_2 in C_2 and the laser head and $(V_1 - V_2)$ in L; b) Peak currents I_{CI} in C_1, I_{C2} in C_2, I_{ZL}in the laser head and I_L in L; and c) Phase delay between V_2 and I_{ZL}.

Figure 3 shows the laser head and the coil power dissipation versus the generator power; to compare these, the generator power is also shown. These power dissipation were calculated using Eq. (5), the voltage and current peak values in Figs. 2a-b, the measured voltage to current phase in the laser head and the calculated voltage to current phase in L (ϕ=89.78°). From Eq. (5), with ϕ=89.999° a power dissipation of 2.4 W for C_2 is calculated when the supplied power is 1 kW. Here the laser power radiation is also shown. Figure 4 shows the calculated capacitive and resistive values in the laser head using Figs. 2a and 2b, and Eqs. (10) and (11). Figure 3 shows that the supplied power in the laser head is from 30 to 40% of the generator power and the difference is lost, about 22 to 33% in the coil L. Also, part of the energy is coupled to the structure of the system (induced proximity effects [30]), producing a temperature rise in the part nearest to L. The rest is dissipated in the other components of the circuit; in fact, at 1 kW, generator power, current, and voltage are under the maximum ratings of C_1, but C_2 works 100% above those and it must be air cooled (under such conditions the system cannot be operated more than 5 minutes). The circuit board used to assemble C_1 and C_2 also dissipate energy, and their temperature rises with the generator power. In particular, the measured resistance of the anode and cathode copper layers of C_2 are about 10 mΩ each one, which account for about 80 W of power dissipation when the system works at 1 kW generator power.

5. Discussion and conclusions

An advantage to exciting CO_2 lasers by capacitive discharges at low frequencies, in comparison to high frequencies ($>$ 13 MHz), could be the lower prices of the electronic equipment involved, particularly the RF power generators. Here we have investigated the operation of a convection

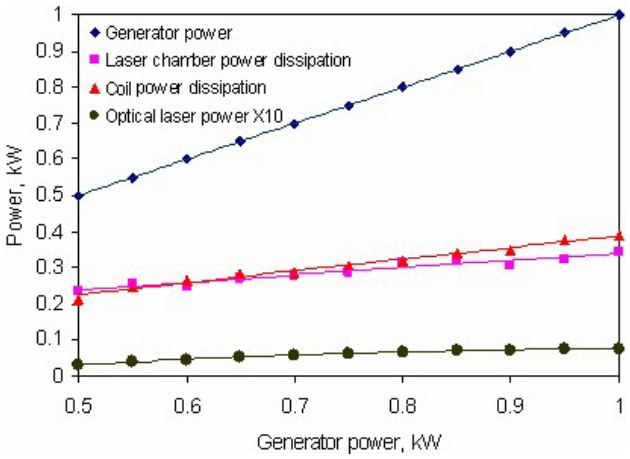

FIGURE 3. Measured laser power and laser head power dissipation as a function of the supplied power. For comparison, the theoretically estimated L power dissipation and the supplied power are also shown.

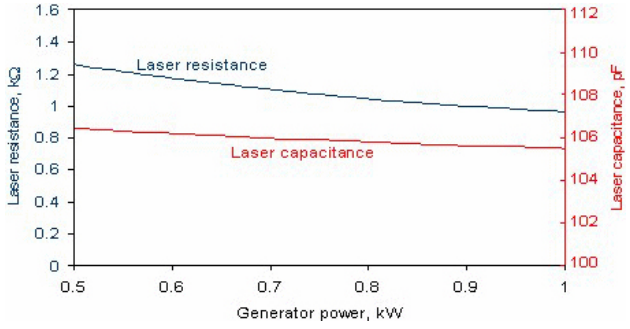

FIGURE 4. Estimated laser head resistance and capacitance as a function of the power supplied.

cooled CO_2 laser excited by a capacitive coupled 450 kHz discharge. Until now, the efficiency obtained (≈0.8%) is 20 times lower than that obtained in slab lasers operated at higher excitation RF frequencies. Another difference is that the voltage applied in our discharge chamber is ten times higher than that applied in slab lasers [31], and so a better electrical isolation is required.

To explain the poor system efficiency, the electrical behavior of the excitation circuit was investigated. It was detected that most of the supplied power in our laser is wasted in heating L, the laser electrodes, the laser tube wall, and the wire used for the interconnections. The total effect is, besides the reduced efficiency of the system, a limited use of the generator power (up to 1 kW). To improve this, it is necessary:

a) to build a coil L with a lower resistance, which could be achieved with silvered copper tube (the conductivity of silver is only 6% better than copper, but when the surface oxidizes, silver oxide is a much better conductor than copper oxide [32]) with larger external and internal diameters, and a ratio of the spacing between adjacent turns to the tube diameter greater than 2, to avoid the direct proximity effects [24];

b) to build a C_2 using more capacitors to support the voltage and current in it and to be in the position to supply the 5 kW maximum power from our RF generator and finally;

c) to avoid the printed circuit board for the assembly of C_1 and C_2, and the circuit element interconnection through wires. Another option for overcoming such problems is to design a RF power generator with output impedances coupled to the discharge chamber impedance, thus avoiding the coupling network.

It is hoped that, by overcoming all the power dissipation problems mentioned above, efficiencies in the order of 20% will be obtained.

Although the measurement of the phase voltage to current in L, C_1 and C_2 with the oscilloscope and the circuit based on the AD8302 were not possible, its measurement in the laser head was made with a 98.5% accuracy. Such measurements are very useful for characterizing the laser head impedance, which is a very important parameter in achieving a model of the laser discharge.

1. P.K. Cheo, *Lasers*, Edited by A.K. Levine and A.J. De Maria (Marcel Dekker Inc., 1971) Vol. 3.
2. W.J. Witteman, *The CO_2 Laser* (Springer Verlag, 1987).
3. *Gas Lasers – Recent Developments and Future Prospects*, Edited by W.J. Witteman and V.N. Ochkin (Kluwer Academic Pub., 1996).
4. Y.P. Raizer, M.N. Shneider and N.A. Yatsenko, *Radio-Frequency Capacitive Discharges* (CRC Press ,1995).
5. *Handbook of the EuroLaser Academy*, Edited by D. Schuöcker (Chapman and Hall 1998) Vol. 1.
6. B. Freisinger, M. Pauls, J.H. Schäfer, and J. Uhlenbusch, *Procc. Of the SPIE* **1397** (1990) 311.
7. A.D. Colley, H.J. Baker, and D.R. Hall, *Appl. Phys. Lett.* **61** (1992) 136.
8. P.P. Vitruk, H.J. Baker and D.R. Hall, J. *Phys. D: Appl. Phys.* **25** (1992) 1282.
9. M.B. Heeman, Y.B. Udalov, K. Hoen, and W.J. Witteman, *Appl. Phys. Lett.* **64** (1994) 673.
10. S. Wieneke, C. Uhrlandt, and W. Viöl, *Laser Phys. Lett.* **1** (2004) 1.
11. J.W. Butterbaugh, L.D. Baston, and H. H.Sawin, *J. Vac. Sci. Technol. A* **8** (1990) 916.
12. L.P. Baker, G.M.W. Kroesen, and F.J. de Hoog, *IEEE Trans. Plasma Sci.* **7** (1999) 759.
13. K. Wiesemann, *On some problems of discharge diagnostics Proceedings of the Frontiers in Low Temperature Plasma Diagnostics V* Meeting 2003.
14. http://fltpd-5.ba.cnr.it/Paper/Libro/1pdf, 27.10.06.
15. J.Y. Montiel and J.M. de la Rosa, *IEEE América Latina* **3** (2005). http://ewh.ieee.org/reg/9/etrans/esp/, 27.10.06.
16. V.A. Godyak, R.B. Piejak, and B.M. Alexandrovich, *IEEE Trans. Plasma Sci.* **19** (1991) 660.
17. C. Beneking, *J. Appl. Phys.* **68** (1990) 4461.
18. J.A.G. Baggerman, R.J. Visser, and E.J.H. Collart, *J. Appl. Phys.* **76** (1994) 738.
19. M.A. Sobolewski and K.L. Steffens, *J. Vac. Sci. Technol. A* **17** (1999) 3281.
20. S. Dine, J. Jolly, and J. Guillon, *Coupled power and plasma impedance measurements in a VHF capacitive discharge in hydrogen*, XXVI International Conference on Phenomena in Ionized Gases 2003-Contributed Papers.http://www.icpig.unigreifswald.de/proceedings/data/Dine_1, 27.10.06
21. B. Walter, *Proc. SPIE* **1020** (1988) 57.
22. Vishay Co. http://www.vishay.com/capacitors, 27.10.06.
23. C. Bowick, *RF circuit design* (W.W. Sams, 1982).
24. S. Ramo, J.R. Whinnery, and T. van Duzer in *Fields and Waves in Communication Electronics* (John Wiley & Sons, 1965).
25. A.W. Lotfi, P.M. Gradzki, and F.C. Lee, *IEEE Trans. Magn.* **28** (1992) 2169.
26. G.L. Johnson, *Solid State Tesla Coil* (2001), http://www.tfcbooks.com/special/sstc_glj.htm, 10.11.06.
27. W. Guo and Ch. A. De Joseph, *Plasma Sources Sci. Technol.* **10** (2001) 43.
28. LF-2.7 GHz, RF/IF Gain and Phase Detector. AD8302, REV. A and REV. O, Analog Devices, www.analog.com, 15.06.06.

29. J. de la Rosa, J. Hamisch, and H.J. Eichler, *J. Phys. D: Appl. Phys.* 21 (1988) 1342.

30. T.M. Roberts and H.D. Hibbert, *Nature* **295** (1982) 42.

31. A. Ducluzaux, *Cahier Technique Schneider Electric* **83** (1983) 1, http://www.schneider-electric.com/cahier_technique/en/pdf/ect83.pdf, 27.10.06

32. S.A. Starostin **et al.**, **Plasma Physics Reports 28** (2002) 63-70.

33. R. Severns, *Conductors for HF Antennas* http://rudys.typepad.com/ant/files/antenna_wire_conductor.pdf, 27.10.06.